articles

molecular pharmaceutics

Modulation of Cell Adhesion Molecules in Various Epithelial Cell Lines after Treatment with PP2†

Anna Maria Calcagno,*,‡,§ Jennifer M. Fostel,∥,⊥ Randal P. Orchekowski,∥,# James T. Alston,∥,▽ William B. Mattes,∥,○ Teruna J. Siahaan,‡ and Joseph A. Ware∥,@

Department of Pharmaceutical Chemistry, The University of Kansas, Lawrence, Kansas 66047, and Pharmacia Corporation, Kalamazoo, Michigan 49007

Received November 4, 2004

Abstract: Regulation and expression of E-cadherin and other adhesion molecules were evaluated after exposure to a selective inhibitor of the Src family of tyrosine kinases and inducer of E-cadherin, PP2. E-cadherin is located within the intercellular junction, and it is involved in the management of paracellular permeability of various epithelial barriers in the body. Epithelial cell lines HCT-116, HT29, Caco-2, LS174T, and ARPE-19 were examined for morphological, functional, protein, and mRNA changes following 20 μM PP2 treatment. PP2 treatment caused cell clustering in Caco-2, HT29, and HCT-116 cells. E-cadherin also redistributed to the points of cell contact in Caco-2 cells. These changes suggest increased E-cadherin-dependent cell adhesion. Studies evaluating transepithelial electrical resistance, an established measurement of paracellular permeability, displayed increases in resistance for the Caco-2 cells following PP2 treatment, which correlates with our microscopy data. In addition, E-cadherin protein levels increased for all cells except HCT-116. ARPE-19 cells did not express E-cadherin at the protein or mRNA level. Expression of adhesion molecules varied for the cell lines, and only Claudin 3 mRNA expression was significantly increased in the three intestinal cell lines treated with PP2. Overall, our data suggest that E-cadherin is positively regulated by inhibition of Src tyrosine kinases at the functional and protein expression levels within these epithelial cell lines.

Keywords: E-cadherin; paracellular drug delivery; adhesion molecules; epithelial cells; PP2; SRC inhibitors

Introduction

The two major routes for drugs to cross biological barriers are the transcellular route and the paracellular pathway. Although many drugs utilize the transcellular route, several limitations exist. First of all, only drugs with the appropriate physiochemical properties can traverse transcellularly.[1] Hydrophilic and charged moieties are unable to use the transcellular path. Second, drugs utilizing the transcellular route must also face efflux transporters as well as various drug metabolizing enzymes before leaving the cell.[2] These conditions severely restrict drug delivery. On the other hand, the passage of hydrophilic drugs through the paracellular pathway is only limited by size. Paracellular drug delivery is regulated by the various adhesion molecules within the intercellular junction. E-cadherin is a critical adhesion molecule located within the adherens junction that organizes epithelial cells into biological barriers.[3] Various factors have

* To whom correspondence should be addressed. Mailing address: Laboratory of Cell Biology, National Cancer Institute, NIH, Building 37, Room 2120, 37 Convent Dr MSC4256, Bethesda, MD 20892-4256. Tel: (301) 435-6303. Fax: (301) 402-0450. E-mail: calcagnoa@mail.nih.gov.

† Presented in part at the American Association of Pharmaceutical Scientists Annual Meeting, October 2003.

‡ The University of Kansas.

§ Presently with the National Cancer Institute, Bethesda, MD 20892.

∥ Pharmacia Corporation.

⊥ Presently with Alpha-Gamma Technologies, Inc., Raleigh, NC 27609.

Presently with The Van Andel Research Institute, Grand Rapids, MI 49503.

▽ Presently with Pfizer Global Research and Development, St. Louis, MO 63141.

○ Presently with Gene Logic, Gaithersburg, MD 20879.

@ Presently with Pfizer Global Research and Development, Ann Arbor, MI 48105.

(1) Martinez, M.; Amidon, G. A mechanistic approach to understanding the factors affecting drug absorption: a review of fundamentals. *J. Clin. Pharmacol.* **2002**, *42* (6), 620−643.

(2) Wacher, V.; Salphati, L.; Benet, L. Active secretion and enterocytic drug metabolism barriers to drug absorption. *Adv. Drug Delivery Rev.* **2001**, *46* (1−3), 89−102.

10.1021/mp0499003 CCC: $30.25
Published on Web 03/08/2005

been shown to be influential in the expression and regulation of E-cadherin.[4,5] Changes in E-cadherin interactions have an impact on the integrity of the epithelial barrier and in turn on the paracellular permeability of small, hydrophilic drugs.[3]

The Src family of kinases, one of the largest and most examined subfamilies of nonreceptor tyrosine kinases, has been identified as a disruptor of E-cadherin-dependent cell−cell adhesions.[6] The Src family consists of nine members, which share a similar structure and common pathways of regulation and function.[7,8] Only three of the nine members of the Src family are found in epithelial cells, and these include Src, Fyn, and Yes, which are ubiquitously expressed.[9] The multiplicity of substrates for Src contains proteins with a variety of functions that either interact directly with Src or have been shown to be phosphorylated in Src transformed cells.[9−11] This list is too large to include here; however, of particular significance are E-cadherin and β-catenin, two important cell adhesion molecules of the adherens junction, which are known substrates of Src. Src phosphorylates the E-cadherin complex and induces its ubiquitination causing a disruption of cell−cell contacts in MDCK cells.[12] Investigators have also shown that inhibition of c-Src increases the adhesive nature of the E-cadherin/catenin complex and inhibits metastasis.[13,14] Recent reports indicate that the pyrazolopyrimidine PP2, a selective inhibitor of the Src family of tyrosine kinases, prevents the Src-dependent phosphorylation of p120 and β-catenin and the subsequent loss of epithelial barrier function during chemical anoxia.[15] PP2 effectively inhibits the Src family members Fyn, Lck, and Hck at nanomolar concentrations in vitro and at higher concentrations in intact cells.[16] Moreover, treatment with 20 μM PP2 resulted in a 40−50% growth inhibition in HT29 cells.[13] PP2 selectively targets the Src family kinases, and it binds to the hydrophobic pocket near the ATP-binding site on the enzyme, which is specific to the Src kinase family.[17] However, this compound also interferes with the catalytic activity of the PDGF receptor at low concentrations, which is not a concern for our work since only the ARPE-19 cells express the PDGF receptor, and no changes were found in our work for this gene following PP2 treatment in the ARPE-19 cells.[18,19]

Although others have evaluated the effects of PP2 in certain epithelial cell lines, our work is a comprehensive study evaluating five epithelial cell lines after exposure to PP2. A comparison of four intestinal cell lines and one retinal epithelial cell line that lacks E-cadherin was performed. Our hypothesis was that intercellular junction regulation of E-cadherin via Src kinases is similar among epithelial cells. In this study, the effects of treatment with 20 μM PP2 for 48 h were evaluated at the morphological, functional, protein, and gene expression levels. This dose regimen was utilized for all studies due to the significant morphological effects that it produced in our preliminary studies for nearly all cell lines after 48 h of treatment. Although our work focuses mainly on the effects on E-cadherin within these cells, we were also able to examine the regulation of genomic expression of thousands of genes following inhibition of Src

(3) Lutz, K. L.; Siahaan, T. J. Molecular structure of the apical junction complex and its contribution to the paracellular barrier. *J. Pharm. Sci*. **1997**, *86*, 977−984.

(4) Fukata, M.; Kaibuchi, K. Rho-family GTPases in cadherin-mediated cell-cell adhesion. *Nat. Rev. Mol. Cell Biol*. **2001**, *2* (12), 887−897.

(5) Aplin, A. E.; Howe, A.; Alahari, S. K.; Juliano, R. L. Signal transduction and signal modulation by cell adhesion receptors: the role of integrins, cadherins, immunoglobulin-cell adhesion molecules, and selectins. *Pharmacol. Rev*. **1998**, *50* (2), 197−263.

(6) Frame, M. C.; Fincham, V. J.; Carragher, N. O.; Wyke, J. A. v-Src's hold over actin and cell adhesions. *Nat. Rev. Mol. Cell Biol*. **2002**, *3* (4), 233−245.

(7) Tatosyan, A. G.; Mizenina, O. A. Kinases of the Src family: structure and functions. *Biochemistry (Moscow)* **2000**, *65* (1), 49−58.

(8) Hubbard, S. R.; Till, J. H. Protein tyrosine kinase structure and function. *Annu. Rev. Biochem*. **2000**, *69*, 373−398.

(9) Thomas, S. M.; Brugge, J. S. Cellular functions regulated by Src family kinases. *Annu. Rev. Cell Dev. Biol*. **1997**, *13*, 513−609.

(10) al-Obeidi, F. A.; Wu, J. J.; Lam, K. S. Protein tyrosine kinases: structure, substrate specificity, and drug discovery. *Biopolymers* **1998**, *47* (3), 197−223.

(11) Brown, M. T.; Cooper, J. A. Regulation, substrates and functions of src. *Biochim. Biophys. Acta* **1996**, *1287* (2−3), 121−149.

(12) Fujita, Y.; Krause, G.; Scheffner, M.; Zechner, D.; Leddy, H. E.; Behrens, J.; Sommer, T.; Birchmeier, W. Hakai, a c-Cbl-like protein, ubiquitinates and induces endocytosis of the E-cadherin complex. *Nat. Cell Biol*. **2002**, *4* (3), 222−231.

(13) Nam, J. S.; Ino, Y.; Sakamoto, M.; Hirohashi, S. Src family kinase inhibitor PP2 restores the E-cadherin/catenin cell adhesion system in human cancer cells and reduces cancer metastasis. *Clin. Cancer Res*. **2002**, *8* (7), 2430−2436.

(14) Owens, D. W.; McLean, G. W.; Wyke, A. W.; Paraskeva, C.; Parkinson, E. K.; Frame, M. C.; Brunton, V. G. The catalytic activity of the Src family kinases is required to disrupt cadherin-dependent cell-cell contacts. *Mol. Biol. Cell* **2000**, *11* (1), 51−64.

(15) Sinha, D.; Wang, Z.; Price, V. R.; Schwartz, J. H.; Lieberthal, W. Chemical anoxia of tubular cells induces activation of c-Src and its translocation to the zonula adherens. *Am. J. Physiol. Renal Physiol*. **2003**, *284* (3), F488−F497.

(16) Hanke, J. H.; Gardner, J. P.; Dow, R. L.; Changelian, P. S.; Brissette, W. H.; Weringer, E. J.; Pollok, B. A.; Connelly, P. A. Discovery of a novel, potent, and Src family-selective tyrosine kinase inhibitor. Study of Lck- and FynT-dependent T cell activation. *J. Biol. Chem*. **1996**, *271* (2), 695−701.

(17) Zhu, X.; Kim, J. L.; Newcomb, J. R.; Rose, P. E.; Stover, D. R.; Toledo, L. M.; Zhao, H.; Morgenstern, K. A. Structural analysis of the lymphocyte-specific kinase Lck in complex with non-selective and Src family selective kinase inhibitors. *Struct. Folding Des*. **1999**, *7* (6), 651−661.

(18) Blake, R. A.; Broome, M. A.; Liu, X.; Wu, J.; Gishizky, M.; Sun, L.; Courtneidge, S. A. SU6656, a selective src family kinase inhibitor, used to probe growth factor signaling. *Mol. Cell. Biol*. **2000**, *20* (23), 9018−9027.

(19) Waltenberger, J.; Uecker, A.; Kroll, J.; Frank, H.; Mayr, U.; Bjorge, J. D.; Fujita, D.; Gazit, A.; Hombach, V.; Levitzki, A.; Bohmer, F. D. A dual inhibitor of platelet-derived growth factor beta-receptor and Src kinase activity potently interferes with motogenic and mitogenic responses to PDGF in vascular smooth muscle cells. A novel candidate for prevention of vascular remodeling. *Circ. Res*. **1999**, *85* (1), 12−22.

family kinases by PP2 through the use of microarray technology. Surprisingly, mRNA expression did not correlate between the studied epithelial cell lines, and only the Claudin 3 gene displayed an increase after treatment for all the intestinal cell lines. In general, inhibition of Src caused an increase in cell adhesion regulated by E-cadherin in most epithelial cell lines. Understanding the influences of Src kinases on the integrity of epithelial barriers is crucial for effective paracellular drug delivery and in the design of specific modulators of this process.

Methods

Cell Culture. The following cell lines were purchased from ATCC (Rockville, MD): ARPE-19, Caco-2, HCT-116, HT29, and LS174T. All cell lines utilized in this work are human epithelial cell lines with adherent growth properties. The ARPE-19 cells are derived from normal retinal pigmented epithelium while the other four cell lines originate from colorectal adenocarcinoma cells. All experiments were performed using cells within 20 additional passages of that received from ATCC. The culture medium for each cell line was made as recommended by ATCC. Media components were purchased from Gibco (Carlsbad, CA). Cells were grown in 150 cm^2 Corning cell culture flasks (Corning, NY) at 37 °C and 5% CO_2. Cells were fed every other day. At confluency, the cells were dissociated with trypsin-EDTA (Gibco) per ATCC subculturing protocol and seeded in 6-well Corning Costar polystyrene plates (Corning) at a density of 1×10^6 cells per well.

Cells were grown for 24 h after seeding in the 6-well plates. A 20 μM PP2 (Calbiochem, San Diego, CA) solution was added to these subconfluent cells at the 24-h mark after seeding (dose 1). The PP2 solution was exchanged 24 h following the first dose (dose 2) and was removed 24 h later. Two doses were administered, and the total exposure time to 20 μM PP2 was 48 h for all cell lines except the Caco-2 cells, which were also treated for 96 h. These dosing schedules were used for the evaluation of protein and mRNA levels following PP2 treatment. In the morphological studies, additional exposure time to PP2 was evaluated. The PP2 was dissolved in DMSO (Sigma, St. Louis, MO) and further diluted with the appropriate medium for each cell line; the final concentration of DMSO was 0.1% for the PP2 and the control medium. Light microscope images of the cells were taken at various time points using a Leica DMRBE microscope (Bannockburn, IL) using a 2.5× Leica lens. Images were captured using a Nikon DXM1200 digital camera (Melville, NY) utilizing the Nikon imaging program Act-1. Adobe Photoshop 7.0 was used to adjust the brightness and contrast of the images.

Confocal Imaging. Caco-2 cells were seeded on Lab-Tek II coverglass chambers, No. 1.5 (Nunc, Rochester, NY), on day zero at a density of 100000 cells per well. After 24 h of growth, either PP2 or the control medium was added to the well and exchanged daily for 96 h of total exposure to 20 μM PP2. The PP2 and control medium were prepared as described in the previous section. Prior to the experiment, the chambers were washed twice with PBS (Gibco) and then blocked for 1 h at room temperature with 10% normal goat serum (Gibco) in PBS. The chambers were then washed twice with PBS. A 1:50 solution of the DECMA-1 clone of the rat anti-mouse E-cadherin antibody (Sigma) in PBS/1% normal goat serum was added to all cell chambers for 1 h at room temperature followed by two washes with PBS. The goat anti-rat Alexa Fluor 488 conjugated antibody (Molecular Probes, Eugene, OR) was incubated with the cells for 30 min at room temperature. This secondary antibody was diluted 1:1000 in PBS/1% normal goat serum. Following two washes with PBS, images were acquired on a LSM510 confocal microscope (Carl Zeiss, Thornwood, NY) with a 25× Plan-neofluor 0.8 numerical aperture lens with the correction collar adjusted for water immersion. Fluorescence was imaged using 488-nm argon laser excitation and a 505-nm long-pass emission filter. The transmitted light image was captured simultaneously in a second detector using differential interference contrast (DIC) optics.

Transepithelial Electrical Resistance (TER) and Mannitol Flux Determination. ARPE-19 and Caco-2 cells were plated on 6-well Corning Costar Transwell plates (Corning, NY) at a density of 1×10^6 cells per well and 650000 cells per well, respectively. Cells were grown for 8 days and allowed to form confluent monolayers prior to treatment with 20 μM PP2, and the transepithelial electrical resistance (TER) was measured on days 4, 7, and 8 with a chopstick apparatus using a voltmeter (Millipore, Bedford, MA). Measurements were taken from three individual monolayers in triplicate for each treatment condition. The TER was determined after subtracting the TER value from the Transwell without cells. The medium with PP2 for the treated cells and medium without PP2 for the control cells were exchanged every 24 h starting on day 9, and the TER was measured daily for several days beginning with day 10 of growth. Statistical analysis was performed using a paired *t*-test and two-factor ANOVA with replication.

A mannitol flux study was performed on the Caco-2 cells following 15 days of growth. The Transwells were washed twice prior to the start of the study. A solution of ^{14}C-radiolabeled mannitol (0.25 μCi/mL in 10 mM HEPES/PBS) was placed on the apical side of the transwell, and the flux over time was determined as the basolateral compartment was sampled and counted using a Packard 1900 CA liquid scintillation analyzer (Palo Alto, CA) at 30, 60, and 120 min. These studies were performed in triplicate.

RNA and Protein Isolation. After 48 h of treatment with 20 μM PP2 or control treatment, RNA and protein were isolated from the 6-well plates. The RNA isolation was performed using the Qiagen Rneasy kit (Valencia, CA) according to the manufacturer's protocol. RNA samples were isolated in duplicate. The total RNA extracts were quantified using a spectrophotometer and Softmax software. The integrity of the RNA was verified using the Agilent 2100 Bioanalyzer (Palo Alto, CA) with the Eukaryote Total RNA assay. The RNA extracts were stored at −80 °C until needed.

Protein was isolated from treated and control wells. The medium was aspirated, and the cells were washed with PBS

(Gibco). Lysis buffer containing 50 mM Tris, pH 7.0, 1% Triton X 100, and one tablet of Complete Mini Protease Inhibitor (Roche, Indianapolis, IN) was then added for 15 min while the plates were kept on ice. The wells were scraped using a Nalgene Nunc No. 23 cell scraper (Rochester, NY) and then transferred to clean vials. The lysate was sonicated before DNase (Qiagen, Valencia, CA) was added. The total protein concentration was determined using a Pierce BCA Protein Assay kit (Rockford, IL). The protein extracts were kept at −80 °C until analyzed in the Western blotting studies.

GeneChip Eukaryotic Expression Arrays. The isolated total RNA was used with the GeneChip Sample Cleanup Module to prepare biotinylated eukaryotic cRNA to hybridize to the GeneChip expression probe arrays according to the manufacturer's protocol (Qiagen). Briefly, double-stranded cDNA was prepared from the isolated RNA using the Invitrogen Life Technologies (Carlsbad, CA) SuperScript system with a T7-$(dT)_{24}$ primer. This double-stranded cDNA was utilized to make the biotin-labeled cRNA by in vitro transcription using a labeling kit from Enzo (Farmingdale, NY). The biotinylated cRNA was fragmented for 35 min at 94 °C in the provided fragmentation buffer and then hybridized to the Affymetrix GeneChip U95Av2 (Santa Clara, CA) arrays for 16 h at 45 °C. The hybridization mixture also contained the following internal controls to ensure hybridization efficiency: control oligonucleotide B2 50 pM, bioB 1.5 pM, bioC 5 pM, bioD 25 pM, cre 100 pM, and herring sperm DNA 0.1 mg/mL. Each probe array was then washed and stained prior to being scanned in duplicate using the GeneArray Scanner according to the manufacturer's procedures (Affymetrix, Santa Clara, CA).

Analysis of GeneChip Data. Affymetrix Microarray Suite 5.0 software was used to examine expression data. The chp data file was analyzed to determine the absent or present call from the detection algorithm, which signifies the absence or presence of a particular mRNA. The signal data were normalized by magnitude adjustment (Fostel and Vidmar, in preparation), and the fold change was determined for the treated and control cells for each of the cell types except for LS174T. A change of 2-fold or more was the criterion for a significant change. The GeneChip data were summarized in the form of a list of changes in gene expression for adhesion molecules from the tight junction, adherens junction, and desmosomes as well as for Src family members. The GeneChip operating software was used to determine the detection call of each of the probes, and the software indicated a "present" call when the transcript was reliably detected or an "absent" call when it was not detected. This was performed using the detection algorithm within the Affymetrix software. These detection calls were used within Table 1 to indicate a change in expression, and a gene was not labeled as present unless a "present" call for each of the duplicate microarrays was found by the GeneChip operating software. A hierarchical clustering using cosine correlation as the distance metric and the complete linkage joining method was performed using Spotfire Functional Genomics software (Somerville, MA).

Western Blotting. Equivalent amounts of protein were prepared under reducing conditions (with NuPage LDS sample and NuPage reducing buffer) and boiled for 2.5 min. A Bio-Rad (Hercules, CA) Criterion precast gel 7.5% Tris-HCl 1.0 mm was used to separate the proteins using SDS−PAGE. One gel was stained with Coomassie blue (Biorad, Hercules, CA) for 20 min and then destained overnight with Bio-Rad destain solution. This Coomassie blue-stained gel verified equal protein loading (data not shown). The Hoefer Easy Breeze drying frame (San Francisco, CA) was used to dry this gel. The electrophoresed proteins from the second gel were transferred to an Immun-Blot PVDF membrane (Bio-Rad); then nonspecific binding was blocked with 5% nonfat dried milk solution (Bio-Rad). The blot was cut in half, and each half was probed with the appropriate antibodies. One half was probed with mouse anti-human E-cadherin antibody (clone 36, Transduction Laboratories, Lexington, KY) at 1:2500 dilution and the other half with mouse anti-actin monoclonal antibody (Chemicon International, Temecula, CA) at 1:8000 dilution overnight at 4 °C with gentle rocking. The secondary antibody, a goat anti-mouse IgG: horseradish peroxidase conjugate (Transduction Laboratories) at 1:5000 dilution, was used for 1 h at room temperature. Amersham Biosciences ECL Western blotting detection reagents (Piscataway, NJ) were used to detect the signal as indicated. The blot was exposed to Hyperfilm within a Hypercassette by Amersham Pharmacia Biotech (Piscataway, NJ) for various times. A Konica SRX-101A film processor (Scarborough, ME) was used to develop the film.

Results

PP2 Causes Morphological Changes and Redistribution of E-Cadherin in Subconfluent Cells. The inhibition of the Src family of tyrosine kinases plays an important role in cell-to-cell adhesion. It has previously been shown that morphological changes occur in HT29 cells following treatment with PP2.[13] We hypothesized that regulation of the intercellular junction would be similar across epithelial cell lines. Our study was performed to determine if PP2 would elicit similar morphological changes in the five epithelial cell lines that we were evaluating. The morphologies of model intestinal cell lines as well as a retinal epithelial cell line were evaluated in subconfluent cells after exposure to 20 μM PP2 for 48 h. In Figure 1, the images of the HCT-116 cells are depicted. In this cell line, the effects of PP2 were seen after only 3 h of exposure (top left panel). The treated cells begin to cluster whereas the control cells continue to spread to form a complete monolayer. No clustering was seen in any of the other cell lines after 3 h, and some differences in cell morphology were seen after 24 h for the treated and control cells for the HCT-116, HT29, and Caco-2 cells (data not shown). The greatest morphological changes were seen after 48 h for all cell lines. After 48 h of treatment with PP2, the differences were more evident for the HCT-116 cells (Figure 1c,d). The treated HCT-116 cells show extensive cell clustering and many spaces between the cells, but the control cells are able to form a complete monolayer.

Table 1. Gene Expression Summary for the Selected Genes[a]

	Caco-2					
	96 h	48 h	LS174T	HCT-116	HT29	ARPE-19
occludin	P	P	P	P	P	P
ZO-3	P	P	P	P	P	A
ZO-2	P	P	P	P	P	P
Claudin 18	A	A	A	A	A	A
Claudin 7	P	P	P	P	P	A
Claudin 5	A	A	A	A	A	A
Claudin 10	A	A	A	A	A	A
Claudin 14	A	A	A	A	A	A
Claudin 8	A	A	A	A	A	A
Claudin 3	P	P +	P	P +	P +	P
Claudin 4	P	P	P	P	P	A
Claudin 9	A	A	A	A	A	A
symplekin	P	P	P	P	P	P
E-cadherin	P	P	P	P	P	A
beta catenin	P	P	P	P	P	P
alpha catenin	P	P	P	P	P	P
p-120 catenin	P	P	P	P	P	P
Iqgap	P	P	P	P	P	P
Rac-1	P	P	P	P	P	P
PI3Kinase	P	P	P	P	P	P
actin alpha	P	P	A	A	A/P	P
actin beta	P	P	P	P	P	P
Rho-A	P	P	P	P	P	P
protein kinase 2 beta	A/P	P	A	P/A	A	A
integrin beta 1	P	P	P	P	P	P
integrin alpha 1	P	P	P	A	P	P −
c-src kinase	P	P	P	P	P	P
actinin alpha 3	A	A	A	A	A	A
actinin alpha2	A	A	A	A	A	A
actinin alpha 1	P	P	P	P	P	P
vinculin	P	P	P	P	P	P
plakoglobin	P	P	P	P	P	P
desmoplakin	P	P	P	P	P +	P
FRK	A	A	A	A	A	A
FGR	A	A	A	A	A	A
YES	P	P	P	P	A/P	P
HGF	A	A	A	A	A	A
SRC	A	P	A	P	P	P
FYN	A	A	A	P/A	P	P
HCK	A	A	A	A	A/P	A
LCK	A	A	A	A	A	A

[a] A = absent, no expression in treated or control cells; P = present, gene expressed in treated and control cells; A/P = absent in PP2-treated and present in the control cells; P/A = present in PP2-treated cells and absent in control cells. + indicates at least a 2-fold increase in expression after treatment with PP2 compared to control cells; − represents at least a 2-fold decrease in expression following PP2 treatment compared to control cells. The Caco-2 data is presented for the 48- and 96-h PP2 treatments. (See Methods section for a more detailed description of the determination of gene expression.)

Cells were evaluated again at the 72-h point, and few changes were seen between the treated cells at 48 and 72 h (data not shown). After 96 h of treatment, a statistically significant difference in the transepithelial electrical resistance was seen in the Caco-2 monolayers. Consequently, this prompted us to assess the morphology of the Caco-2 cells and the distribution of E-cadherin in these cells after 96 h of treatment. The Caco-2 cells treated with PP2 for 96 h also show a clustering effect. The control cells, depicted in Figure 2B, are a confluent monolayer. The LS174T cells do not show the same response as the other cells after incubation with PP2. These cells were found not viable following 48-h incubation with 20 μM PP2. The control LS174T cells continue to spread to form a monolayer and show a slow growth rate, which was normal for this particular cell line (Figure 2C,D).

Figure 3 displays the morphological changes in the HT29 and ARPE-19 cells. The HT29 cells form cell clusters after treatment with PP2 as previously reported by other investigators.[13] The control cells for HT29 formed a confluent

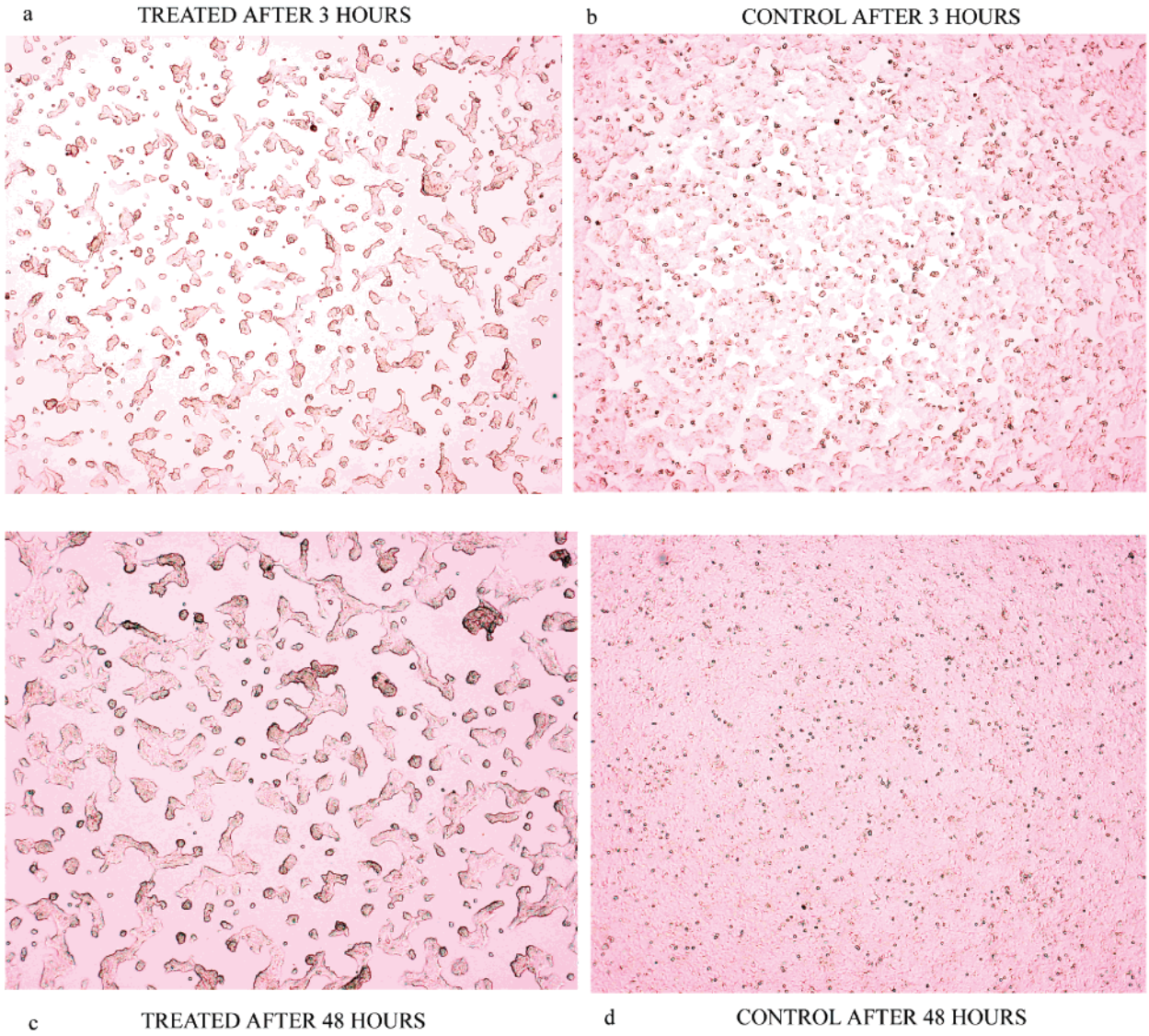

Figure 1. Light microscopy images of HCT-116 cells. (a) This image, captured after 3 h of treatment with 20 μM PP2, depicts the early stages of cell clustering in subconfluent cells. (b) The control HCT-116 cells at 3 h are seen in this panel. Cells are spreading to form a monolayer. (c) HCT-116 cells after 48 h of PP2 treatment show more defined cell clusters. (d) These control cells of HCT-116 after 48 h have formed a complete monolayer. (Magnification of 2.5× for all images.)

monolayer after 48 h of growth. The ARPE-19 treated and control cells (Figure 3c,d) showed no visual difference when imaged by light microscopy.

As mentioned previously, the functional changes in the Caco-2 cells following 96 h of treatment with PP2 triggered further evaluation of these cells. To determine if these changes were attributable to E-cadherin, additional microscopy studies were performed. The distribution of E-cadherin in the Caco-2 cells was examined by confocal microscopy following 96 h of treatment with 20 μM PP2 (Figure 4 z-stack flat image). The control cells grew as a thin monolayer of cells over the entire surface of the Lab-tek II chamber, and the immunostaining with the DECMA-1 clone of the anti-E-cadherin antibody shows a diffuse staining over the surface of the cells. The diffuse staining was apparent throughout the slices of the z-stack performed on this sample (Figure 5 depicts z-stack full image). The PP2-treated Caco-2 cells formed a cluster of cells with a greater thickness than that of the control cells, and the E-cadherin staining was more intense on the borders of the cells as seen in the fluorescent image and throughout the z-stack (Figure 5). These data suggest that this clustering is a result of cells growing on one another and of the redistribution of E-cadherin to the points of cell contact inhibiting cell motility, which is necessary for the spread of cells and the formation of monolayers.

PP2 Exposure Results in Changes in Paracellular Permeability in Confluent Monolayers. Functional characterization of these cells after treatment with PP2 was performed using transepithelial electrical resistance (TER) and mannitol flux evaluation to determine paracellular permeability in confluent monolayers. These measurements were taken to determine if PP2 treatment would result in a decrease in paracellular permeability due to an increase in cell to cell adhesion. The results of these studies are illus-

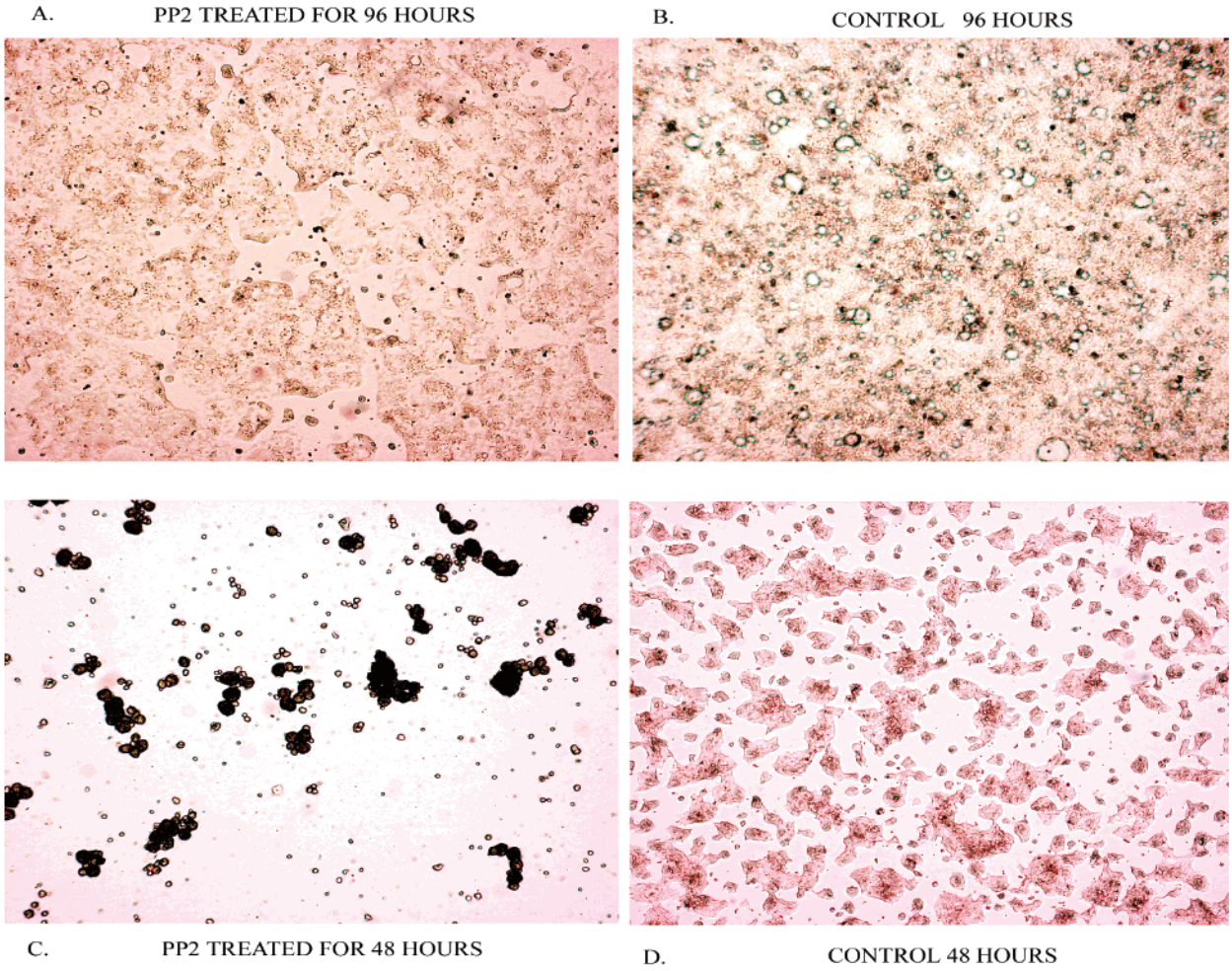

Figure 2. Light microscopy images of Caco-2 cells. (A) Subconfluent Caco-2 cells treated for 96 h with PP2 fail to form a complete monolayer, and cell clusters are seen. (B) Control Caco-2 cells form a confluent monolayer after 96 h of growth. (C) LS174T cells treated with PP2 were found to be not viable after 48 h of treatment. (D) Control LS174T cells after 48 h continue to spread to form a monolayer. (Magnification of 2.5× for all images.)

trated in Figure 6. The Caco-2 cells were chosen for these studies because they are model intestinal cells that develop into tight monolayers. Conversely, the ARPE-19 cells form looser monolayers with lower TER values than the Caco-2 cells, and they lack E-cadherin in the early stages of their growth. The other cell lines in this study did not form monolayers with measurable TER values; thus, they are not useful for evaluating paracellular permeability in this manner.

The ARPE-19 confluent monolayers (Figure 6a) show a decrease in TER following treatment with 20 μM PP2 compared to the control cells. The average TER for the control cells ($n = 3$) on day 8 was $147.5 \pm 31.6\ \Omega{\cdot}cm^2$, and it continued to increase to nearly $180 \pm 23\ \Omega{\cdot}cm^2$ over the next 6 days. A statistically significant difference ($p < 0.01$) was observed on day 11 between control cells and cells treated for 48 h with PP2. The TER was measured through day 14 of growth, and the trend continued for the remainder of the study. Statistically significant differences ($p < 0.01$) were found between PP2-treated and control monolayers and between the TER values determined on the five treatment days using a two-factor ANOVA with replication.

The opposite was detected in the Caco-2 confluent monolayers (Figure 6b). PP2 treatment produced an increase in TER for the Caco-2 monolayers with a statistically significant difference ($p < 0.01$) found on day 12 of growth after 96 h of treatment. The average TER for the control cells was $830 \pm 51\ \Omega{\cdot}cm^2$ for the course of the study ($n = 3$). The increase in TER continued for the treated cell monolayers throughout the study. The ANOVA indicated that there was a statistically significant difference ($p < 0.01$) between the treated and control monolayers. At day 15 of growth, the Caco-2 cells were used to further evaluate the paracellular permeability with a mannitol flux assay. Mannitol flux results show that $Pe = 4.07 \times 10^{-7} \pm 3.64 \times 10^{-8}$ for PP2-treated cells and $Pe = 2.48 \times 10^{-7} \pm 1.84 \times 10^{-8}$ for control monolayers ($n = 3$). In each case, the effective permeability was low; however, the control cells display statistically significantly less permeability ($p < 0.05$).

E-Cadherin Protein Expression Is Increased in Two Cell Lines Following PP2 Treatment. As a result of our previous findings that E-cadherin redistributes to the points of cell contact and that cell adhesion is enhanced, we

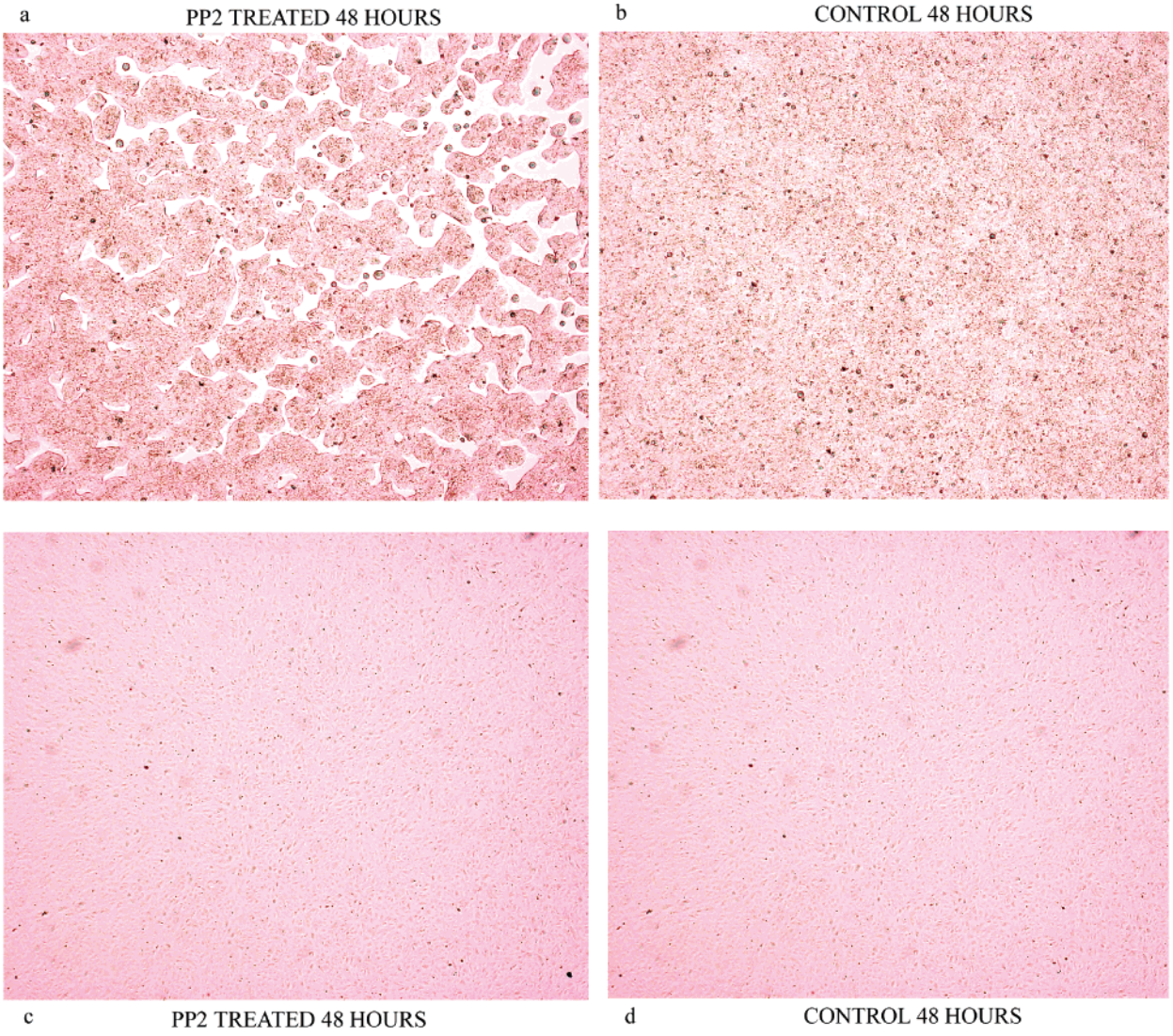

Figure 3. Light microscopy images of subconfluent HT29 and ARPE-19 cells. (a) HT29 cells treated for 48 h with PP2 form cell clusters. (b) After 48 h, control HT29 cells formed a complete monolayer. (c) ARPE-19 cells treated for 48 h with PP2 are depicted. (d) Control ARPE-19 cells after 48 h of growth are shown. No visible differences can be found between panels c and d. (Magnification of 2.5× for all images.)

determined whether PP2 would cause any alterations in the expression of E-cadherin. Total protein was isolated from the various treated and control cells, and the levels of E-cadherin protein expression were compared (Figure 7). The E-cadherin expression level was normalized to the actin control for each cell line. The E-cadherin signal for the PP2-treated cells was approximately half that of the HCT-116 control cells. The cellular levels of E-cadherin were increased for the treated HT29 cells and the Caco-2 cells treated for 48 and 96 h. The HT29 cells showed an increase of 50%, which was similar to the results for the Caco-2 cells treated for 96 h. The Caco-2 cells treated for 48 h showed the greatest increase in E-cadherin protein expression. On the other hand, no E-cadherin signal was detected for either the treated or control ARPE-19 cells, respectively (see lanes 9 and 10 in Figure 7).

Gene Expression Analysis Shows an Increase in Claudin 3 mRNA Levels for Three of the Intestinal Cell Lines Treated with PP2. Since its inception, great advances have been made in oligonucleotide microarray technology. Its rapid development was triggered by the joining of photolithography and solid-phase synthesis to produce the GeneChip, which can interrogate a complex mixture in a highly

(20) Fodor, S. P.; Read, J. L.; Pirrung, M. C.; Stryer, L.; Lu, A. T.; Solas, D. Light-directed, spatially addressable parallel chemical synthesis. *Science* **1991**, *251* (4995), 767−773.
(21) Fodor, S. P.; Rava, R. P.; Huang, X. C.; Pease, A. C.; Holmes, C. P.; Adams, C. L. Multiplexed biochemical assays with biological chips. *Nature* **1993**, *364* (6437), 555−556.
(22) Chee, M.; Yang, R.; Hubbell, E.; Berno, A.; Huang, X. C.; Stern, D.; Winkler, J.; Lockhart, D. J.; Morris, M. S.; Fodor, S. P. Accessing genetic information with high-density DNA arrays. *Science* **1996**, *274* (5287), 610−614.
(23) Lipshutz, R. J.; Fodor, S. P.; Gingeras, T. R.; Lockhart, D. J. High-density synthetic oligonucleotide arrays. *Nat. Genet.* **1999**, *21* (Suppl. 1), 20−24.

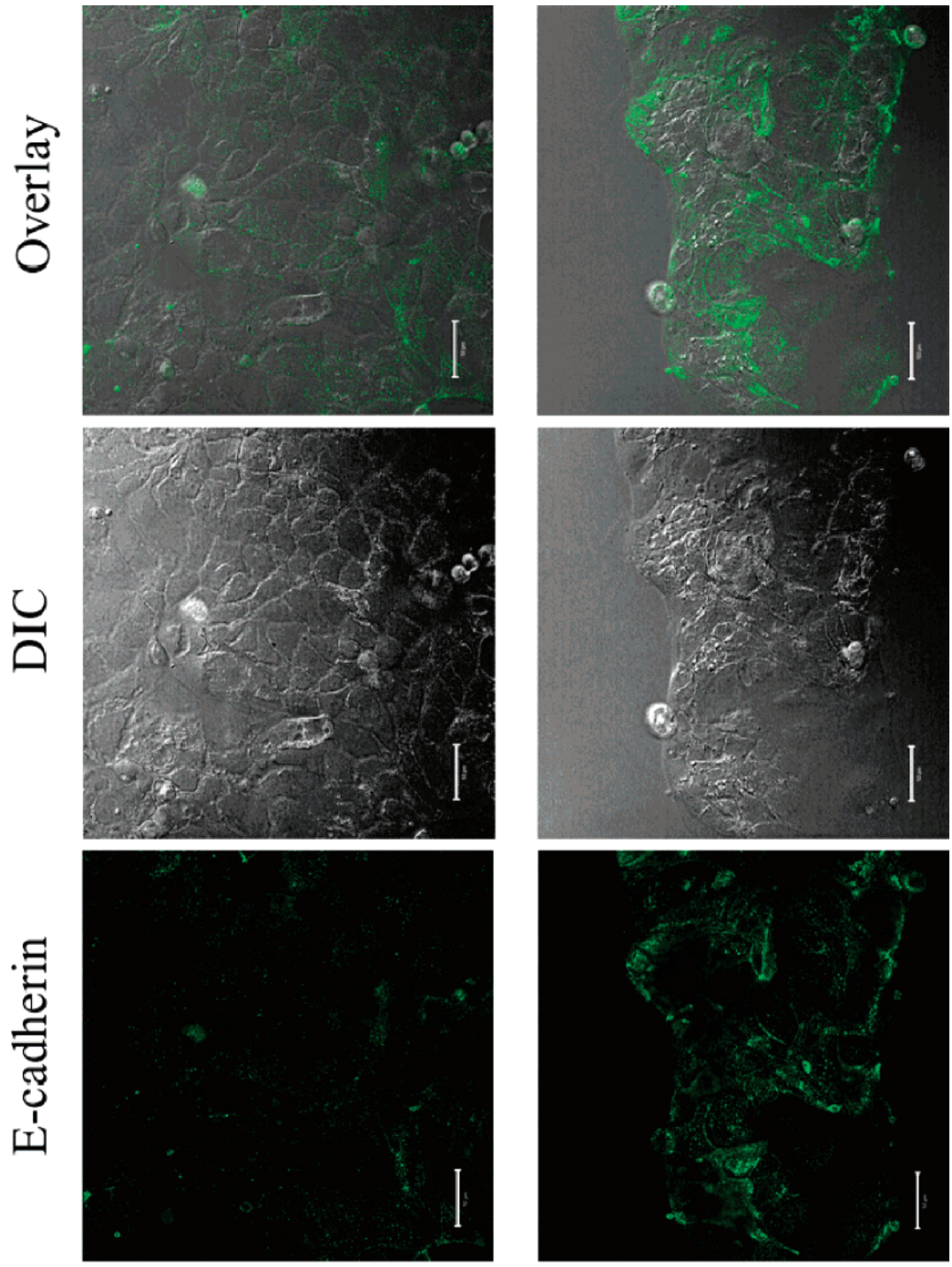

Figure 4. Confocal images of Caco-2 cells. Subconfluent Caco-2 samples were imaged on a confocal microscope following 96 h of treatment. This figure depicts the flat z-stack image. Top panels depict the control sample, while the bottom panels represent the PP2-treated samples. Green corresponds to anti-E-cadherin staining. The differential interference contrast (DIC) panel is the corresponding transmitted light image of the fluorescence panel. Images shown are from the same experiment taken with identical instrument settings for comparative purposes and are representative of separate experiments. Contrast was enhanced and the figure composed using Adobe Photoshop. The bar represents 50 μm in all panels.

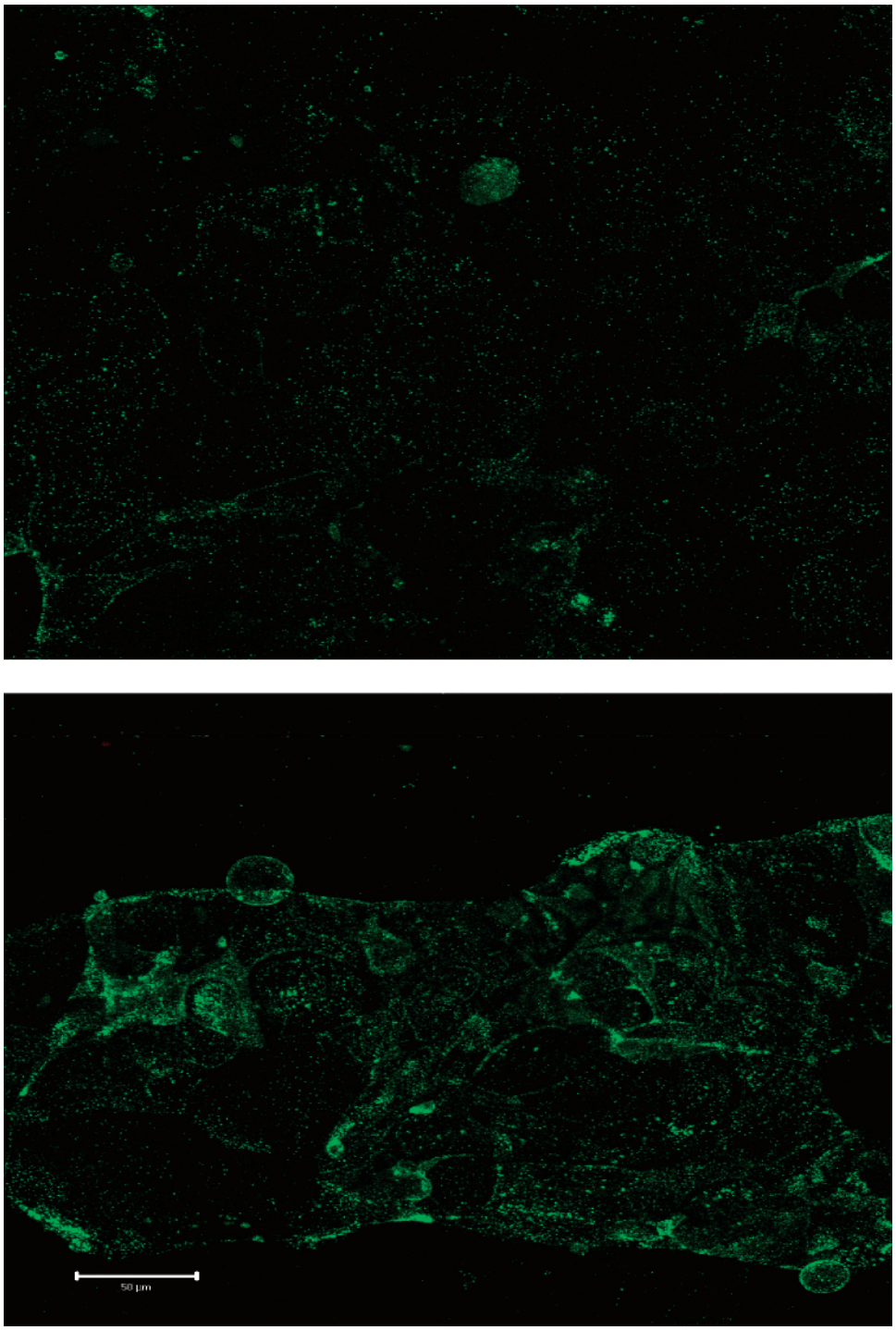

Figure 5. The top panel is the full z-stack image of the control sample, and the bottom panel shows the PP2-treated sample in the full z-stack image. The bar represents 50 μm.

parallel manner.[20−23] This robust technology was the perfect choice for the evaluation of the effects of this Src kinase inhibitor on the gene expression of several human adherent epithelial cell lines. The effects on each individual cell line as well as a comparison of all cell lines were evaluated. Due to the cytotoxicity of PP2 in the LS174T cells, only the control cells were analyzed with microarrays.

The hierarchical clustering, a popular technique for clustering microarray data, is presented in Figure 8. This indicates the patterns in gene expression profiles across the different experimental conditions. The dendrogram representing the experimental conditions shows that three major groups were found. Clusters are formed for the cell lines which show similar gene expression for all the probe sets (>12000) on the microarray. The Caco-2 cells, which were treated for 48 and 96 h, as well as the controls for each condition were clustered to form the first group. The next group was made up of the remaining intestinal cell lines, indicating

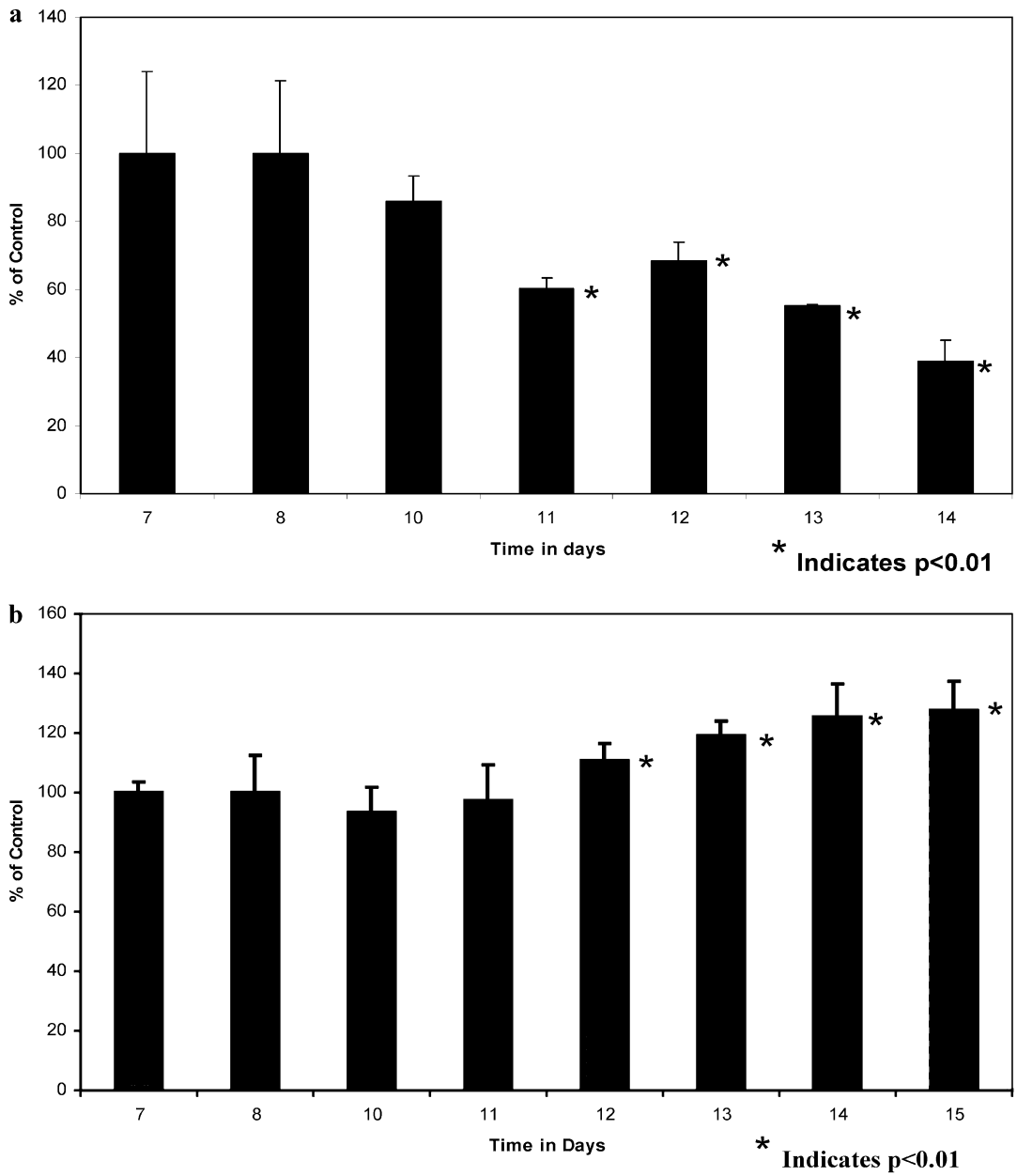

Figure 6. Transepithelial electrical resistance (TER) responses to PP2 exposure. (a) ARPE-19 confluent monolayers show a decrease in TER following treatment with PP2. (b) Confluent monolayers of Caco-2 cells treated with PP2 show an increase in TER after 96 h of treatment. PP2 (20 μM) was added to the confluent monolayers after 9 days of growth and exchanged daily thereafter. TER values of PP2-treated cells ($n = 3$) were compared to TER values of control cells ($n = 3$) and presented as % of control. The statistically significant difference between the control and treated samples was determined using a paired *t*-test for each time point.

that these cell lines have similar gene expression patterns. The last group contains the ARPE-19 retinal epithelial cells. First of all, the dendrogram shows that the gene expression patterns for the treated and control Caco-2 cells are unrelated to those of the other three intestinal cell lines as the Caco-2 cells form their own cluster. This occurrence is quite surprising. This dendrogram also displays that for all experimental conditions the duplicate microarrays form clusters, indicating that that the results were reproducible. Interestingly, the PP2-treated results for a given cell line always formed a larger cluster with its untreated controls. This suggests that the PP2 treatment did not change gene expression so dramatically across all the probe sets for these cell lines.

After normalizing the data by magnitude adjustment, analysis was begun by searching for trends in the data. Profiles were searched using the Spotfire software, and no uniform response was displayed to the treatment with PP2 in the epithelial cell lines studied. Table 1 displays the expression data for a list of adhesion molecules from the tight junction, adherens junction, and desmosomes, regulators of cell−cell adhesion, and the Src family members. This chart indicates expression of the genes for each cell type and any

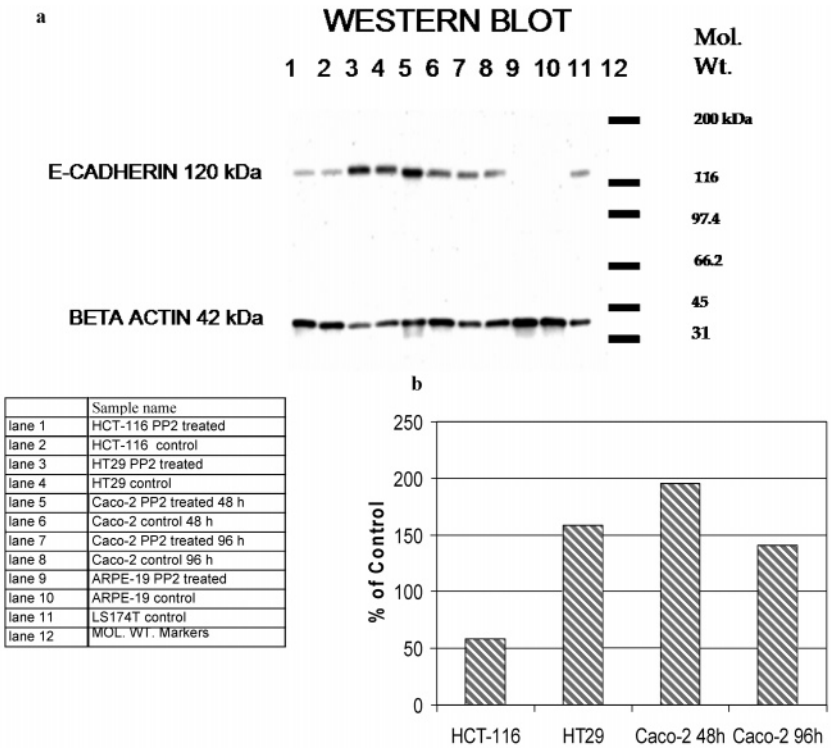

	Sample name
lane 1	HCT-116 PP2 treated
lane 2	HCT-116 control
lane 3	HT29 PP2 treated
lane 4	HT29 control
lane 5	Caco-2 PP2 treated 48 h
lane 6	Caco-2 control 48 h
lane 7	Caco-2 PP2 treated 96 h
lane 8	Caco-2 control 96 h
lane 9	ARPE-19 PP2 treated
lane 10	ARPE-19 control
lane 11	LS174T control
lane 12	MOL. WT. Markers

Figure 7. Western blot for E-cadherin (120 kDa) and beta actin (42 kDa) after PP2 treatment. (a) The total protein loaded was 4.5 μg per lane. The legend below indicates the samples present within each lane. No signal was detected for E-cadherin in lanes 9 and 10, which corresponds to the ARPE-19 samples. (b) The comparison of the E-cadherin signal for control and treated cells is presented in this graph. HCT-116 cells show a decrease in total E-cadherin after PP2 treatment for 48 h. Increases in protein levels of E-cadherin were seen in HT29 cells treated for 48 h, Caco-2 cells treated for 48 h, and Caco-2 cells treated with PP2 for 96 h.

significant changes in expression. An "A" represents absence and no expression, while "P" indicates presence and gene expression. A 2-fold change was used as the criterion for significant gene expression changes. Treatment with PP2 did cause some changes in gene expression within these cells; however, most changes were less than the 2-fold criterion. Claudin 3 showed a 2-fold increase after treatment with PP2 in the HCT-116, HT29, and Caco-2 cells treated for 48 h. In the HT29 cells, desmoplakin also showed an increase in expression following treatment with PP2. In the ARPE-19 cells, there was a 2-fold decrease in expression in integrin alpha 1.

For certain genes, exposure to the PP2 caused their gene expression to be absent, although expression was detected in control cells for these genes. A designation of A/P was used, indicating that the gene was absent for the treated cells yet present for the control cells. Alpha actin, YES, and HCK are three genes that displayed this behavior in the HT29 cells. Protein kinase 2 beta is another gene in Caco-2 cells treated for 96 h that was absent after treatment. The HCT-116 cells exhibited the opposite effect for protein kinase 2 beta and FYN in which exposure to PP2 caused gene expression to occur, designated as P/A.

Discussion

Many compounds have been tested for selective inhibition of the Src family members.[24,25] Cell type dictates the

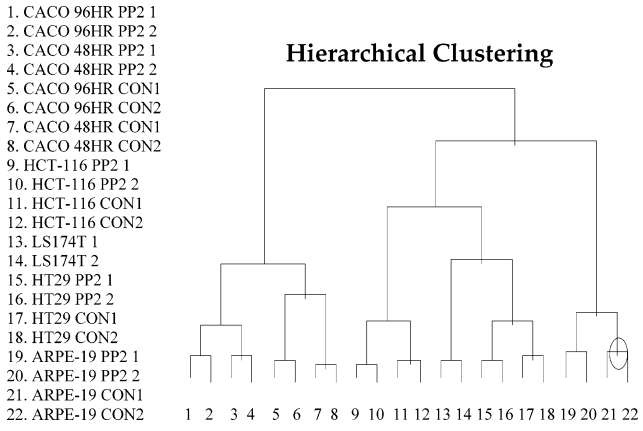

Figure 8. Hierarchical clustering of all microarrays using cosine correlation as the distance metric and the complete linkage joining method. Hierarchical clustering using cosine correlation as the distance metric and the complete linkage joining method was performed using Spotfire Functional Genomics software to identify patterns in the microarray data, whereby three groups demonstrated significantly different gene expression profiles. Cell lines with similar gene expression patterns are clustered together to form a group. Group one, located on the left, contains all the Caco-2 treatments. Group two consists of the remaining intestinal cell lines, and the last group is the ARPE-19 cells. The numbers below the dendrogram indicate the sample identification.

expression of Src family members; several Src kinases are expressed ubiquitously.[9] PP2 has been shown to be a potent and selective inhibitor of several Src family members at nanomolar ranges in vitro and low micromolar concentrations in intact cells; however, PP2 cannot differentiate between the various members of the Src family.[16] Investigators have shown that treatment with 20 μM PP2 caused 40−50% growth inhibition in HT29 cells.[13] These factors prompted the use of 20 μM PP2 in our studies to investigate the effects in several other epithelial cell lines. All subconfluent intestinal epithelial cells treated with PP2 showed similar patterns in cell clustering when examined with light microscopy. The retinal epithelial cell line, ARPE-19, did not show any morphological changes after PP2 treatment. This suggests that the effects of PP2 may not be similar in all epithelial cell lines at this concentration and dose schedule. This phenomenon has been reported previously by other investigators as Src effects have been shown to be cell-type specific. In particular, in primary keratinocytes isolated from double knockout mice for Src and Fyn, cell adhesion is defective, indicating the same type of role for Src and Fyn in adhesion processes.[26] PP2 was found to be cytotoxic to the LS174T cells. This observation is consistent with the effects of Src inhibitors in other cell lines. Inhibitors of Src cause inhibition of cell growth and the induction of apoptosis in A431 cells;[27] mitotic arrest was reported in breast cancer cell lines following treatment with another selective tyrosine kinase inhibitor.[28] Recent studies report that the inhibition of both focal adhesion kinase (FAK) and Src leads to apoptosis in colon cancer cells.[29] Our microarray data suggests that the LS174T cells express the lowest amount of FAK compared to the other intestinal cell lines and that PP2 treatment causes FAK to increase in expression in the other intestinal cell lines. It is possible that the LS174T cells may be more susceptible to apoptosis or mitotic arrest due to the low expression of FAK, which induces PI3K-AKT dependent anti-apoptotic pathways; however, the exact mechanism is unknown at this time.

PP2 effects on E-cadherin were further investigated by confocal microscopy. Caco-2 cells treated for 96 h with PP2 showed a redistribution of E-cadherin to the points of cell contact. Cells grew as a thick cluster whereas the control cells formed a thin monolayer with diffuse staining of E-cadherin. Similar results were reported in human epidermal keratinocytes treated with the tyrosine kinase inhibitor, PD162531.[14] ARPE-19 control cells were also immunostained with the E-cadherin antibody DECMA-1 after 7 days of growth (data not shown); however, a very low fluorescence signal was obtained even at the highest concentrations of antibody. The lack of morphological changes seen in the ARPE-19 cells, the lack of staining for E-cadherin, and the lack of a signal for E-cadherin in the Western blot and microarray studies indicate that E-cadherin was not present within these cells including those grown for 7 days. Differentiation of ARPE-19 cells occurs within 3−4 weeks after reaching confluency.[30] Previous investigators report that E-cadherin expression occurs in late confluence in cells that already express N-cadherin and only in a subset of epithelioid cells;[31] therefore, E-cadherin would not be expected to be found in our cells. The ARPE-19 cells have been a useful tool in understanding the importance of E-cadherin in the inhibition of Src.

The increase in TER in confluent Caco-2 monolayers with the inhibition of Src is consistent with the increase in cell adhesion. The decrease in the ARPE-19 cells may be due to a decrease in N-cadherin which is constitutively expressed in these cells regardless of confluency time and since E-cadherin is not present. The mRNA levels of N-cadherin decreased by 2.3-fold after treatment with PP2, and no other adhesion molecule expressed in ARPE-19 cells shows a significant change in expression. The mannitol flux data is not consistent with the increase in TER for the Caco-2 cells; however, flux assays are not as sensitive to small changes in permeability, and they possess lower time resolution compared to TER measurements.[32] It has been reported that changes in TER do not always correlate with flux studies.[32,33] Changes in the intercellular space where E-cadherin is located can cause a change in TER, which reflects the resistance of both the tight junction and intercellular space. For the flux assay, the tight junction serves as the first barrier for the permeation of mannitol, and changes in the intercellular space may not affect the permeability of the tight junction. The control cells show less paracellular permeability than the

(24) Lawrence, D. S.; Niu, J. Protein kinase inhibitors: the tyrosine-specific protein kinases. *Pharmacol. Ther.* **1998**, *77* (2), 81−114.
(25) Bain, J.; McLauchlan, H.; Elliott, M.; Cohen, P. The specificities of protein kinase inhibitors: an update. *Biochem. J.* **2003**, *371* (Part 1), 199−204.
(26) Calautti, E.; Grossi, M.; Mammucari, C.; Aoyama, Y.; Pirro, M.; Ono, Y.; Li, J.; Dotto, G. P. Fyn tyrosine kinase is a downstream mediator of Rho/PRK2 function in keratinocyte cell-cell adhesion. *J. Cell Biol.* **2002**, *156* (1), 137−148.
(27) Karni, R.; Levitzki, A. pp60(cSrc) is a caspase-3 substrate and is essential for the transformed phenotype of A431 cells. *Mol. Cell Biol. Res. Commun.* **2000**, *3* (2), 98−104.
(28) Moasser, M. M.; Srethapakdi, M.; Sachar, K. S.; Kraker, A. J.; Rosen, N. Inhibition of Src kinases by a selective tyrosine kinase inhibitor causes mitotic arrest. *Cancer Res.* **1999**, *59* (24), 6145−6152.
(29) Golubovskaya, V. M.; Gross, S.; Kaur, A. S.; Wilson, R. I.; Xu, L.-H.; Yang, X. H.; Cance, W. G. Simultaneous Inhibition of Focal Adhesion Kinase and Src Enhances Detachment and Apoptosis in Colon Cancer Cell Lines. *Mol. Cancer Res.* **2003**, *1* (10), 755−764.
(30) Dunn, K. C.; Aotaki-Keen, A. E.; Putkey, F. R.; Hjelmeland, L. M. ARPE-19, a human retinal pigment epithelial cell line with differentiated properties. *Exp. Eye Res.* **1996**, *62* (2), 155−169.
(31) Burke, J. M.; Cao, F.; Irving, P. E.; Skumatz, C. M. Expression of E-cadherin by human retinal pigment epithelium: delayed expression in vitro. *Invest. Ophthalmol. Visual Sci.* **1999**, *40* (12), 2963−2970.
(32) Yap, A. S.; Mullin, J. M.; Stevenson, B. R. Molecular analyses of tight junction physiology: insights and paradoxes. *J. Membr. Biol.* **1998**, *163* (3), 159−167.
(33) Mitic, L. L.; Anderson, J. M. Molecular architecture of tight junctions. *Annu. Rev. Physiol.* **1998**, *60*, 121−142.

treated cells. This also suggests that the effects of inhibiting Src are less prominent when the cells are more mature. Studies indicate that endocytosis of E-cadherin is decreased in confluent MDCK II cells compared to preconfluent cells.[34]

Protein expression levels of E-cadherin are increased in HT29 and Caco-2 cells following treatment with PP2. Nam et al. reported similar results for HT29 cells.[13] It is possible that the inhibition of Src prevents the internalization of E-cadherin and its subsequent proteolysis. PP2 treatment may also cause transcriptional activation of E-cadherin or its posttranslational modifications. Further studies are necessary to determine which mechanism is responsible for the increase. In the HCT-116 cells, there is a decrease in the total protein levels of E-cadherin. Our microarray data for HCT-116 shows a decrease of nearly 1.5-fold in gene expression for α-catenin. Studies by Hinck et al. show that adhesion can be restored in human lung cancer cells which lack α-catenin but express E-cadherin by transfecting α-catenin into these cells.[35] This suggests that the interaction between E-cadherin and α-catenin is vital for cell−cell adhesion. A decrease in α-catenin would cause E-cadherin to be easily removed from the lateral surface of the cells because there would be no linkage to the actin cytoskeleton.

Differences in cell types may account for the decrease in this cell line. The effects of PP2 may not be as prevalent in this cell line after prolonged exposure. As mentioned previously, the ARPE-19 cells would not be expressing E-cadherin at this stage of their growth, and this was found in the Western blot results.

Inhibition of the Src family of tyrosine kinases by PP2 produced very few changes at the gene expression level for the adhesion molecules studied. A 2-fold change was used as the guideline for significant changes. Others have reported an increase in E-cadherin mRNA expression in HT29 cells after treatment with PP2.[13] In this work, there was a small increase in E-cadherin expression in the HT29 cells; however, it is far less than the 2-fold criterion. For the other intestinal epithelial cells studied, no changes were found in the genomic expression of E-cadherin. The results of E-cadherin mRNA expression in these three intestinal cell lines were confirmed by SYBR-green real-time PCR (data not shown). The LS174T data is included in Table 1, although it represents only the expression level in the control cells and not the comparison of treated and control as in the other cell lines due to the cytotoxicity of PP2 to the LS174T cells. The ARPE-19 cells show no mRNA expression of E-cadherin after 48 h of growth; this again confirms the results of the Western blotting. The differences in mRNA and protein levels of E-cadherin for the other cells could be due to various circumstances, including posttranslational modifications, degradation, posttranslational splicing, and messenger stability.[36]

Only one adhesion molecule, Claudin 3, showed such an increase for all the intestinal cell lines treated with PP2 for 48 h. There was no change, however, in the gene expression of Claudin 3 in ARPE-19 cells. Claudin 3, a component of the tight junctions consisting of four transmembrane domains, was recently discovered.[37] The importance of the claudin family in the regulation of the tight junctions has recently been demonstrated. Investigators have shown that the three membrane associated guanine kinases (MAGUKs), ZO-1, ZO-2, and ZO-3, are still recruited to the tight junctions in occludin-deficient mice and that these MAGUKs, which cross-link the tight junctional proteins to the actin filaments, also bind to the carboxy terminal of claudins in addition to binding to occludin.[38] Introduction of Claudin 2 into MDCK I cells converted these cells into a more permeable or leaky cell type; however, no decrease in paracellular permeability was reported when Claudin 3 was added.[39] This indicates that expression of Claudin 3 may increase cell adhesion. Thus, our findings suggest a possible relationship between Src inhibition and Claudin 3 expression. Phosphorylation plays a critical role in the interactions within the tight junction. Tyrosine phosphorylation of ZO-1 increases following oxidative stress, and studies implicate this tyrosine phosphorylation in disrupting the interaction between the occludin−ZO-1 complex and actin cytoskeleton, leading to an increase in paracellular permeability.[40] The exact relationship between Claudin 3 and Src family members is yet to be established; however, this work suggests that one might exist.

Desmoplakin in the HT29 cells also showed an increase in expression after exposure to PP2. Desmoplakin interacts with plakoglobin within the desmosomes, and plakoglobin is a known substrate of the Src family of tyrosine kinases.[11] This increase in expression suggests the possibility that the

(34) Le, T. L.; Yap, A. S.; Stow, J. L. Recycling of E-cadherin: a potential mechanism for regulating cadherin dynamics. *J. Cell Biol*. **1999**, *146* (1), 219−232.

(35) Hinck, L.; Nathke, I. S.; Papkoff, J.; Nelson, W. J. Dynamics of cadherin/catenin complex formation: novel protein interactions and pathways of complex assembly. *J. Cell Biol*. **1994**, *125* (6), 1327−1340.

(36) Celis, J. E.; Kruhoffer, M.; Gromova, I.; Frederiksen, C.; Ostergaard, M.; Thykjaer, T.; Gromov, P.; Yu, J.; Palsdottir, H.; Magnusson, N.; Orntoft, T. F. Gene expression profiling: monitoring transcription and translation products using DNA microarrays and proteomics. *FEBS Lett*. **2000**, *480* (1), 2−16.

(37) Morita, K.; Furuse, M.; Fujimoto, K.; Tsukita, S. Claudin multigene family encoding four-transmembrane domain protein components of tight junction strands. *Proc. Natl. Acad. Sci. U.S.A.* **1999**, *96* (2), 511−516.

(38) Itoh, M.; Furuse, M.; Morita, K.; Kubota, K.; Saitou, M.; Tsukita, S. Direct binding of three tight junction-associated MAGUKs, ZO-1, ZO-2, and ZO-3, with the COOH termini of claudins. *J. Cell Biol*. **1999**, *147* (6), 1351−1363.

(39) Furuse, M.; Furuse, K.; Sasaki, H.; Tsukita, S. Conversion of zonulae occludentes from tight to leaky strand type by introducing claudin-2 into Madin-Darby canine kidney I cells. *J. Cell Biol*. **2001**, *153* (2), 263−272.

(40) Rao, R. K.; Basuroy, S.; Rao, V. U.; Karnaky Jr, K. J.; Gupta, A. Tyrosine phosphorylation and dissociation of occludin-ZO-1 and E-cadherin-beta-catenin complexes from the cytoskeleton by oxidative stress. *Biochem. J*. **2002**, *368* (Part 2), 471−481.

stabilization of plakoglobin requires a greater supply of desmoplakin for interactions with the intermediate filaments.

Table 1 also lists one other regulator of cell adhesion that changed expression levels. This is integrin alpha 1, which shows a decrease in ARPE-19 cells. Integrins are able to activate Src kinases which, in turn, phosphorylate proteins involved in integrin-mediated events; investigators also have shown that Src can function as a scaffold to regulate signaling of integrins.[41] This suggests that the inhibition of Src may decrease the amount of integrin needed. In regard to the genes that were either turned on or turned off by PP2 treatment, it has been suggested that various genes show transcription that is positively or negatively regulated by v-Src. Various transcriptional control elements have been implicated in Src's transcriptional activation.[3]

The actions of the Src family of tyrosine kinases influence a variety of functions within the body, including cell adhesion. Recent discoveries have implicated Src in the endocytosis of E-cadherin since the phosphorylation by Src triggers the E-cadherin complex to be ubiquitinated by Hakai and endocytosed in MDCK cells, a model canine epithelial cell.[12] Hakai has been shown to interact only with E-cadherin, and studies indicate that this interaction is dependent on tyrosine phosphorylation.

Regulation of the E-cadherin complex plays a critical role not only in cell adhesion but also in metastasis, cell invasion, and wound healing. Inhibition of Src in human epidermal keratinocytes results in enhanced cell adhesion through E-cadherin even in low calcium concentrations; yet it inhibits wound repair in vitro.[14] Src, Fyn, and Yes are all present within the adherens junction. At this time, the disruption of cell−cell adhesion at the adherens junction cannot be attributed to a particular member of the Src family.[14] Owens et al. have shown that the catalytic activity of one or more of these endogenous Src members is necessary to disassociate cadherin interactions at the adherens junction.[14] Studies in Caco-2 cells show that oxidative stress induces activation and translocation of Src.[42] This results in the phosphorylation of components of the tight and adherens junctions and the dissociation of the tight junctions, which increases paracellular permeability.

Treatment of epithelial cells with a selective inhibitor of the Src family of tyrosine kinases resulted in increased cell adhesion in the intestinal cell lines. Caco-2, HT29, and HCT-116 cells displayed cell clustering and compaction, indicating increased cell adhesive properties. E-cadherin redistributed to the points of cell contact in Caco-2 cells following PP2 treatment. Decreases in TER in ARPE-19 cells following PP2 treatment may be attributed to the lack of E-cadherin expression at the early stages of cell growth or possibly the decrease in another junctional protein. On the other hand, Caco-2 cells exhibited higher TER values after PP2 treatment, suggesting that the junctional components, including E-cadherin, were enhanced. The total protein levels of E-cadherin increased for all cells except HCT-116, which showed a decrease. The lack of expression of E-cadherin at the protein or mRNA level of the ARPE-19 cells confirmed earlier reports that these cells do not express E-cadherin at early growth stages. The ARPE-19 cells do not express E-cadherin after 48 h of growth; however, they do express other adhesion molecules. The expression of the adhesion molecules varied for the cell lines studied, and only Claudin 3 showed a significant increase in three of the cell lines treated with PP2. These studies suggest that Src may regulate the expression of this claudin family member although additional work is necessary to understand this relationship. Cell type is an important factor in the expression levels of adhesion molecules after treatment by PP2. The exact relationship between E-cadherin and the Src family of tyrosine kinases needs to be elucidated; however, on the basis of these results, it seems reasonable to conclude that Src is crucial for the regulation of cell adhesion in epithelial cells.

Acknowledgment. We thank Dr. Joseph A. Vetro, Dr. Karen L. Leach, and Dr. James Christensen for critically reviewing this manuscript and providing useful suggestions. We thank Pharmacia Corporation for providing A.M.C. the internship opportunity. A.M.C. was supported by the AFPE Predoctoral Fellowship, a Merck Tuition Fellowship, and the Pharmacia Internship Program. This work was also supported by funding from NIH grants (GM-08359 and EB-00226). We thank Nancy Harmony for her help in preparing this manuscript.

MP0499003

(41) Cary, L. A.; Klinghoffer, R. A.; Sachsenmaier, C.; Cooper, J. A. SRC catalytic but not scaffolding function is needed for integrin-regulated tyrosine phosphorylation, cell migration, and cell spreading. *Mol. Cell. Biol.* **2002**, *22* (8), 2427−2440.

(42) Basuroy, S.; Sheth, P.; Kuppuswamy, D.; Balasubramanian, S.; Ray, R. M.; Rao, R. K. Expression of Kinase-inactive c-Src Delays Oxidative Stress-induced Disassembly and Accelerates Calcium-mediated Reassembly of Tight Junctions in the Caco-2 Cell Monolayer. *J. Biol. Chem.* **2003**, *278* (14), 11916−11924.